Supporting information

Insights into molecular mechanism underlying carbon fixation inhibition of rice induced by Cadmium

Xinru Zhang[1, 2], Jie Chen[1, 2], Jianjian Wu[3], Wei Wang[1, 2], Lizhong Zhu (✉)[1, 2]

1 College of Environmental and Resource Sciences, Zhejiang University, Hangzhou 310058, China

2 Zhejiang Provincial Key Laboratory of Organic Pollution Process and Control, Hangzhou 310058, China

3 College of Environment and Resources, Xiangtan University, Xiangtan 411105, China

Contents

✉ Corresponding author

E-mail: zlz@zju.edu.cn

Text S1 Determination of Cd Concentrations in Rice Tissues

About 0.1 g of rice tissue powders were digested by aqua regia (30% hydrogen peroxide (H_2O_2) to 65% nitric acid (HNO_3), 1:4, *v*/*v*) with WX-6000 microwave system (PreeKem Scientific Instruments Co., Ltd., Shanghai, China) at 180℃ for 40 min. After microwave digesting, the samples were diluted with 2% HNO_3 (*w*/*w*) to a volume of 5 mL. The contents of Cd in plant tissues were measured by the Inductive Coupled Plasma Mass Spectrometry (iCAP RQ ICP-MS, Thermo Fisher, MA, USA). The recovery rates and detection limit of Cd for all samples were 91.3% − 105.7% and 1 ng/g, respectively.

Text S2 Fluorescence spectroscopy detection

Rubisco protein (2 μmol/L) was combined with different concentrations of Cd^{2+} and incubated for 30 min at 298K or 310K. Excitation and emission slits of 5 nm were used in all measurements. The fluorescence value of the buffer solution (0.01 mol/L PBS solution, pH 7.2–7.4) was taken as the blank throughout the measurements. The fluorescence value of the buffer solution was recorded to eliminate background noise. All measurements were repeated three times, and the mean value was used. Quenching of Rubisco protein by high concentrations of Cd^{2+} in solution was quantified by fitting a Stern-Volmer equation where K_{SV} is the Stern-Volmer quenching constant and K_q is the bimolecular quenching rate constant (Eq. (S1)):

$$F_0/F = 1 + K_{SV}[Q] = 1 + K_q\tau 0[Q] \quad (S1)$$

where F_0 represents the intrinsic fluorescence intensity of Rubisco, F represents the fluorescence intensity of protein with different concentrations of Cd^{2+}, [Q] represents the concentration of Cd^{2+} of quench agent, and τ0 represents the fluorescence lifetime of protein without quench agent (generally 10^{-8} s).

K_a, the effective quenching constant for fluorophores was calculated by the modified Stern-Volmer equation (Eq. (S2)):

$$F_0/(F_0\text{-}F) = 1/f_aK_a[Q] + 1/f_a \quad (S2)$$

where the F_0 and F are the fluorescence intensities before and after a quencher addition, respectively, f_a is the fraction of fluorescence, and [Q] is the concentration of Cd^{2+}.

Text S3 Circular dichroism (CD) spectroscopy

Rubisco protein was diluted with distilled water to the concentration of around 5 μmol/L. After incubation at room temperature for 30 min, the secondary structure of Rubisco-Cd^{2+} conjugates were analyzed in a 1 cm path-length quartz cuvette by a circular dichroism (CD) spectrophotometer (J-1700, Jasco, Japan) at 190 − 260 nm with a scanning speed of 50 nm/min. The data were scanned three times per spectrum. The background spectrum of distilled water was subtracted throughout the measurements. The measured CD spectral data are expressed in millidegrees (mdeg).

Text S4 Measurement of Cd and Mg after spin filtration

For ICP-MS analysis, samples were diluted using trace metal grade HNO_3 to a final concentration of 6% nitric acid. The samples were heated in an oven at 80℃ overnight, cooled to room temperature, and analyzed by ICP-MS. Cd^{111} and Mg^{23} concentrations in the samples were derived from an external calibration curve generated by a series of dilutions of atomic absorption standard (Fluka Analytical) prepared in the same 6% HNO_3 matrix as the samples. All buffers are routinely analyzed for metal content using ICP-MS. Because Milli-Q water is employed to prepare all buffers, we do not typically observe the presence of metals above the lower limit of quantitation. If we do observe detectable levels of metal in the buffer, the buffer is discarded and remade.

Text S5 Measurements of 3-PGA and 2-PG using LC-MS/MS

Quantification of products formed upon Rubisco-catalyzed reactions was carried out on a Waters Xevo TQ MS ACQUITY UPLC system (Waters, Milford, MA, USA) with an Atlantis Premier BEH Z-HILIC column (100 mm × 2.1 mm, 1.7 μm particle size, Waters, Milford, MA, USA). Mobile phase A was 15 mmol/L ammonium hydroxide in water (pH = 9.0), and mobile phase B was 90:10 acetonitrile: water containing 15 mmol/L ammonium hydroxide (pH = 9.0). The gradient elution program is shown in the Table S2. Mass spectrometric detection was completed by use of an electrospray ionization (ESI) source in negative ion multiple-reaction monitoring

(MRM) mode. Samples were normalized using the internal standard, ribitol. The ESI ion source parameters are presented in Table S3. The ion-pair information was shown in Fig. S1.

Text S6 Determination of Rubisco activity

The content and activity of Rubisco in rice leaves under the treatment of Cd were determined using ELISA kits. First, 50 μL of different concentrations of standards were added into standard wells; 10 μL of sample supernatants and 40 μL of sample diluent were mixed as the tested samples. Then, 100 μL of enzyme reagent was added to each well and was incubated at 37℃ for 60 min. Afterwards, the samples were discarded and the plates were washed using the provided washing solution for at least five times. Clean the residual solution in the sample wells by tapping gently. Next, 50 μL of colorant A and 50 μL of colorant B were added to the sample wells, shaking gently to mix them thoroughly and incubating at 37℃ for 15 min. After that, 50 μL of termination solution was used to terminate the reaction. Finally, the absorbance of samples was measured at 450 nm using an enzyme marker instrument (Tecan Infinite® M1000 Pro, Switzerland).

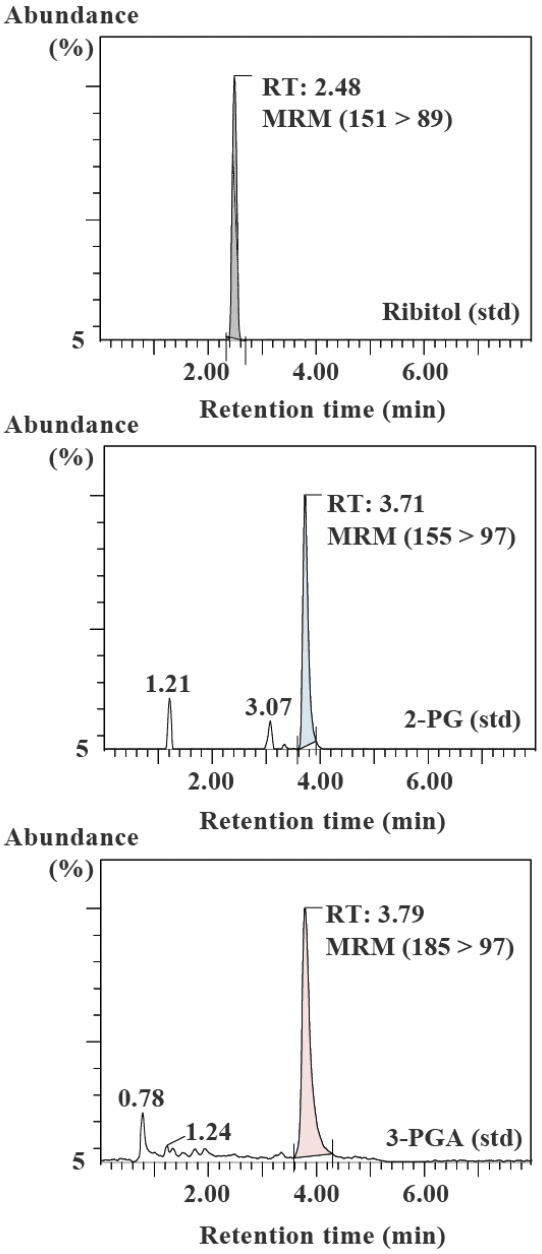

Fig. S1 Mass chromatograms of Ribitol, 2-PG, and 3-PGA obtained under MRM mode of LC-MS/MS.

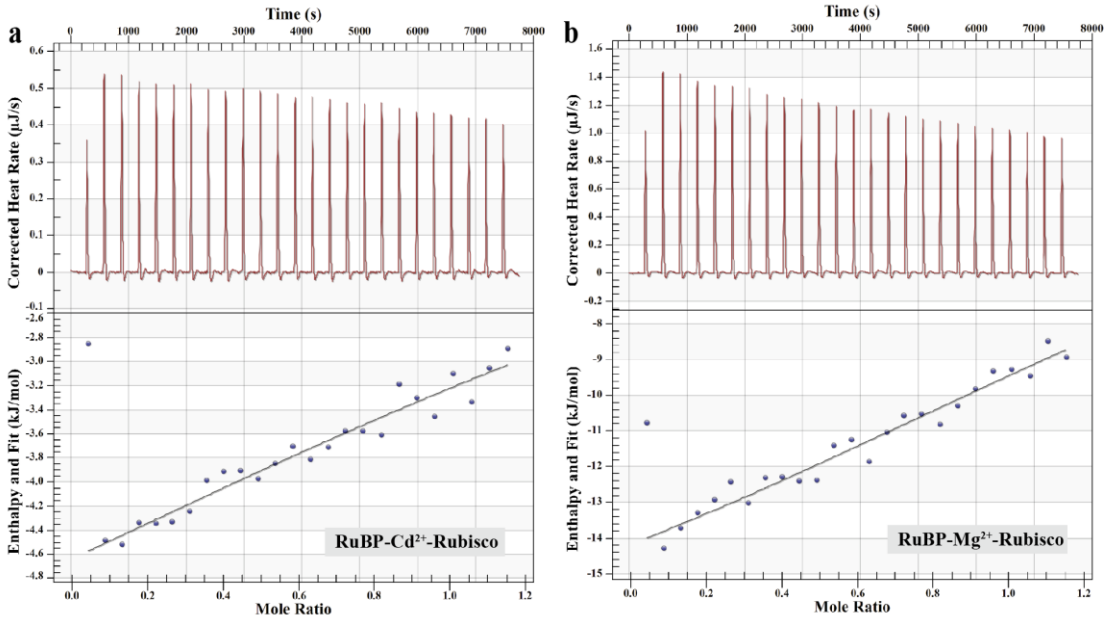

Fig. S2 ITC graph for the titration of RuBP to Cd^{2+}-Rubisco (a) and Mg^{2+}-Rubisco (b). The ligand injection profile (Top) and the calculated heat/enthalpy change for each ligand injection (Bottom) are shown in the graph.

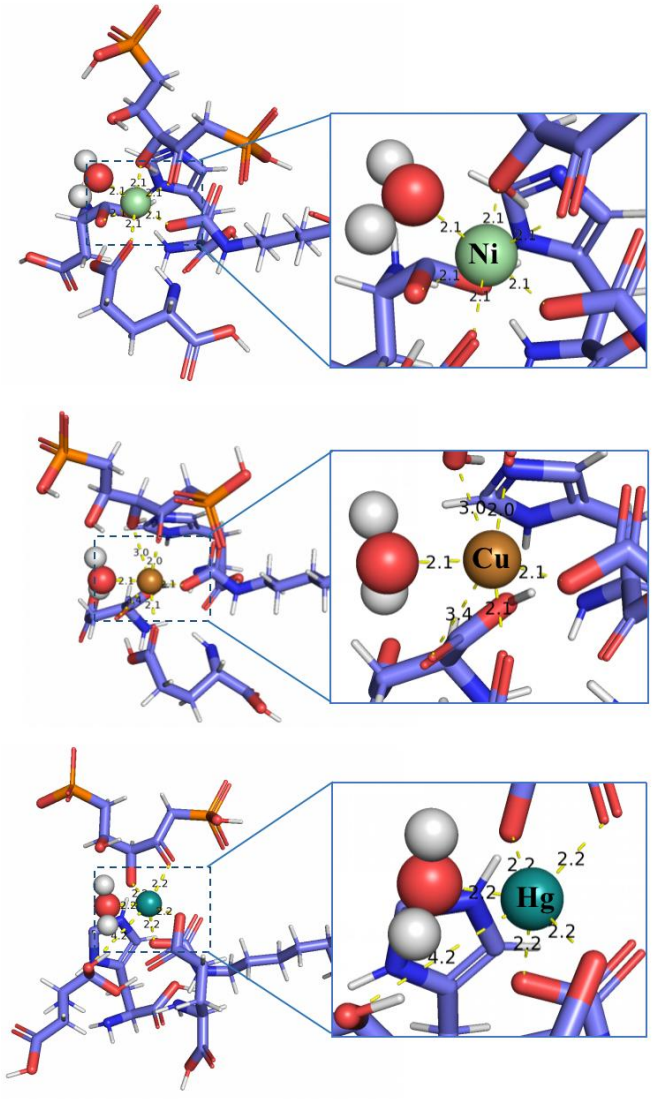

Fig. S3 Binding modes between three divalent metal ions (Ni^{2+}, Cu^{2+}, and Hg^{2+}) and Rubisco.

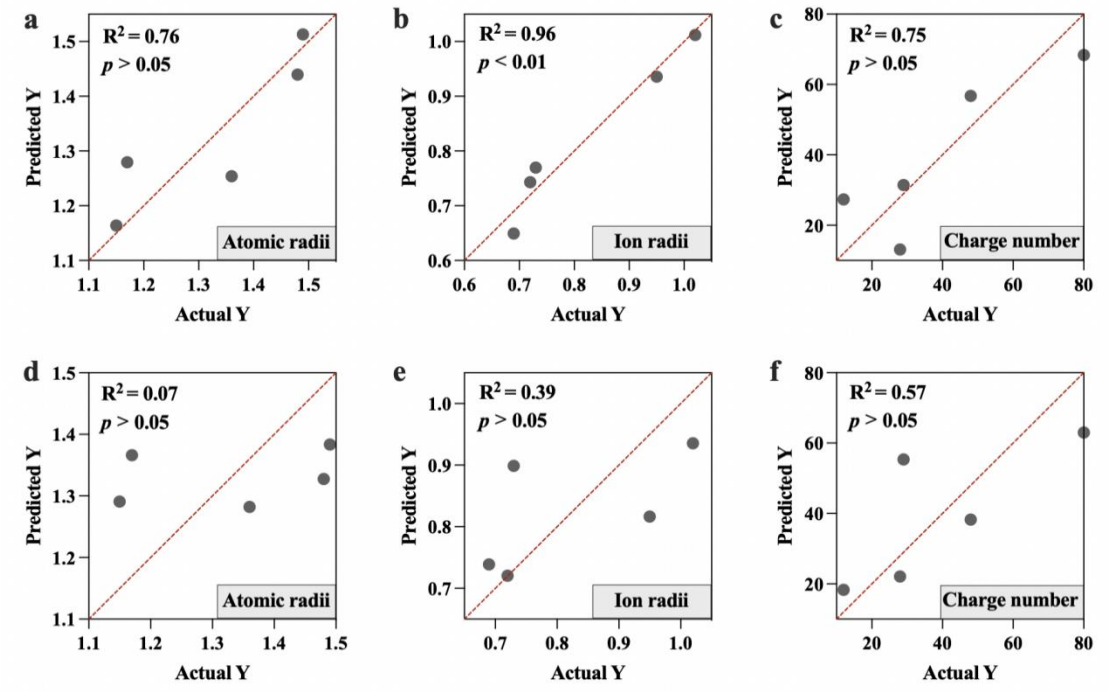

Fig. S4 Correlation analysis between metal ionic properties and binding affinity. R^2 and *p* values are indicated in each graph. The linear regression analysis between binding energy and atomic radii (a), ion radii (b), charge number (c); the linear regression analysis between bond length and atomic radii (d), ion radii (e), charge number (f).

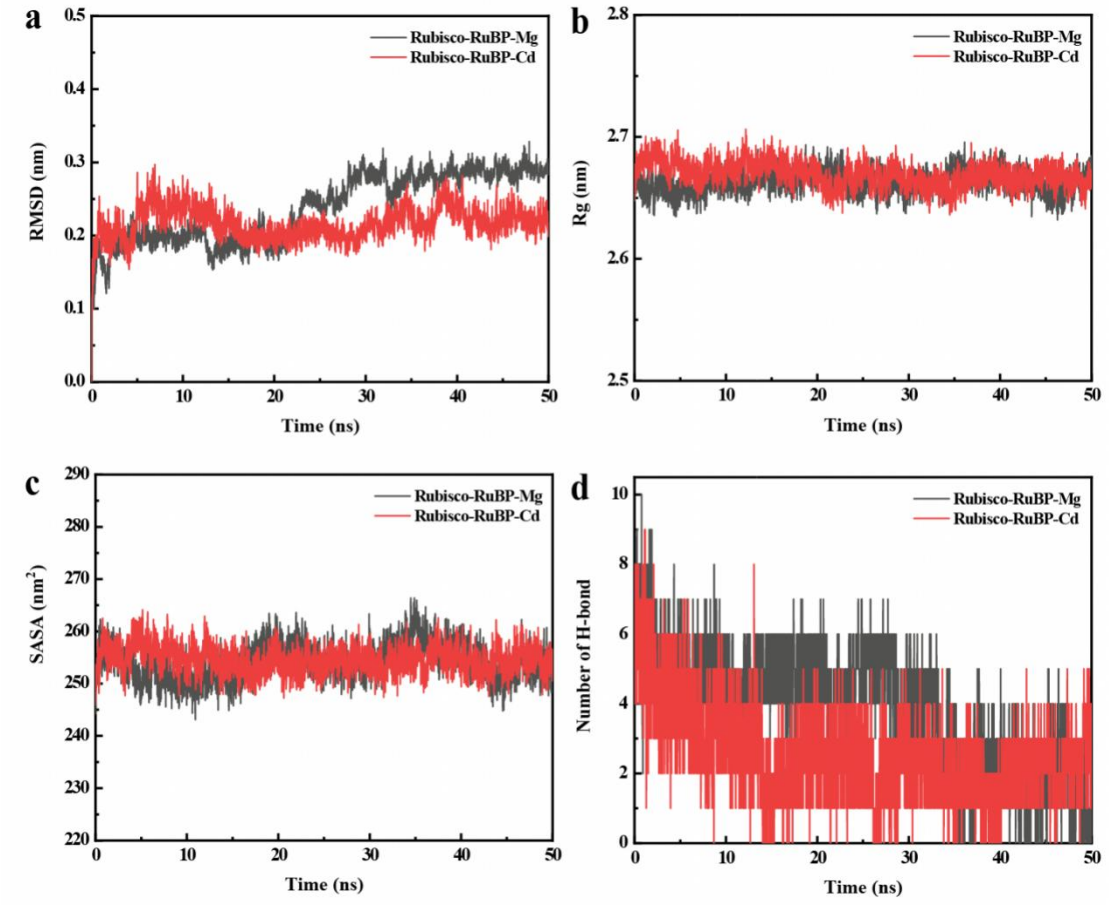

Fig. S5 Structural stability, dynamic behavior, and solvent interactions of complexes in MD simulations. RMSD (a), Rg (b), SASA (c), Number of H-bond (d) of Cd^{2+}-Rubisco-RuBP and Mg^{2+}-Rubisco-RuBP.

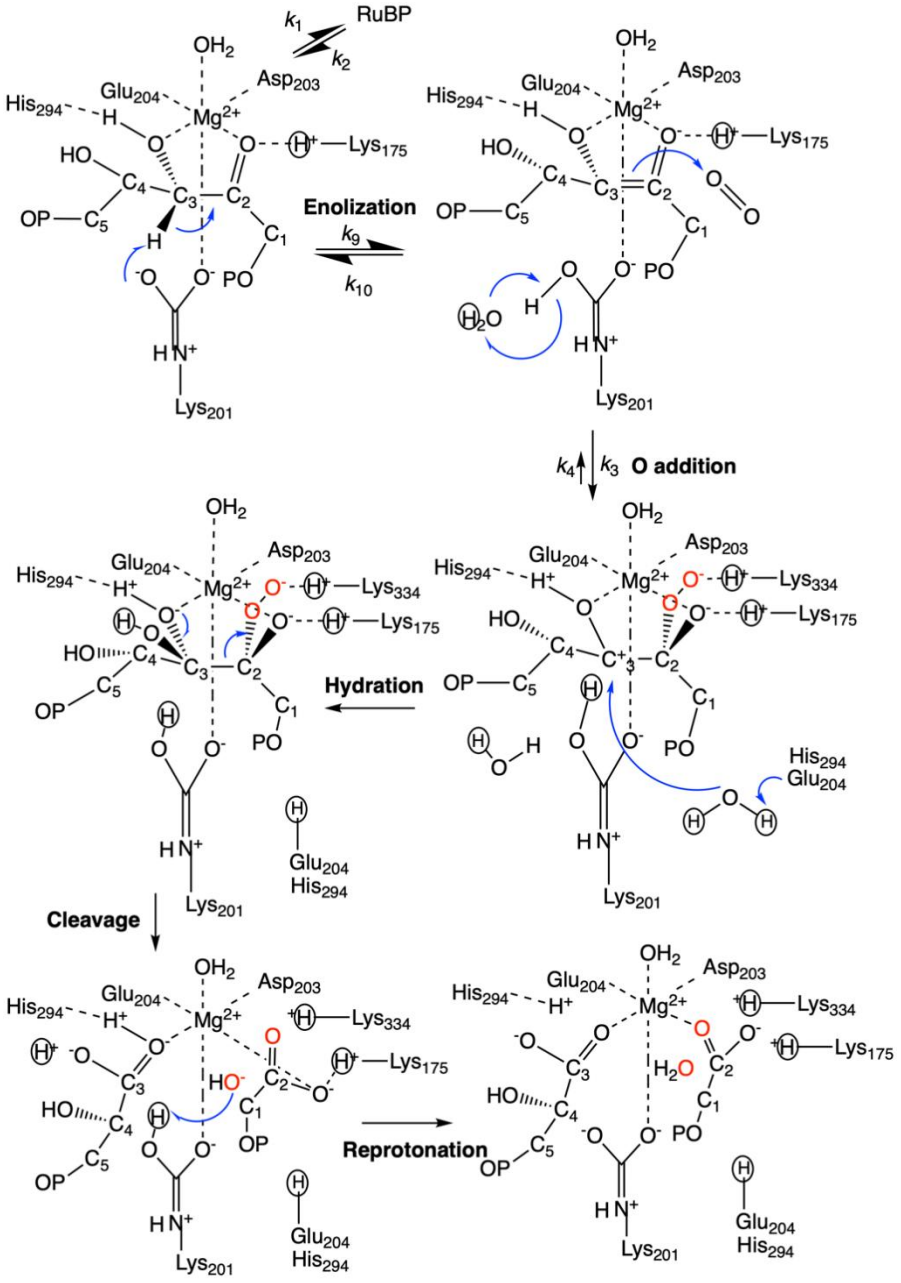

Fig. S6 Hypothetical mechanism associated with Rubisco-catalyzed oxygenation of RuBP. Rate constants are indicated using the notation k_i. Residue numbering refers to the spinach enzyme. The origin of protons is shown with different symbols (circled H for solvent-derived protons, z-shaped arrow for His294-attached proton and bold H for the C3 proton of RuBP). Phosphate groups are represented with the letter 'P'. Here, O_2 and H_2O addition are represented as separate events (stepwise mechanism), but they may be concerted; if so, k_3 would be a combination of O_2 and H_2O addition and k_5 would only include proton exchange and cleavage.

Table S1 Compositions of Hoagland's solution.

Nutrient element	Compositions	Concentration (mg/L)
N	NH_4NO_3	114.30
P	$NaH_2PO_4 \cdot 2H_2O$	50.30
K	K_2SO_4	89.20
Ca	$CaCl_2$	157.00
Mg	$MgSO_4 \cdot 7H_2O$	410.00
Si	$Na_2SiO_3 \cdot 9H_2O$	568.00
Mn	$MnCl_2 \cdot 4H_2O$	1.79
Mo	$(NH_4)_6Mo_7O_{24} \cdot 2H_2O$	0.09
B	H_3BO_3	1.13
Zn	$ZnSO_4 \cdot 7H_2O$	0.04
Cu	$CuSO_4 \cdot 5H_2O$	0.04
Fe	Fe-EDTA-$Na_2 \cdot 3H_2O$	30.00

Table S2 Liquid phase separation gradient for the liquid chromatography mobile phase.

Time (min)	Flow rate (mL/min)	Solvent A (%)	Solvent B (%)	Profile
0	0.3	10	90	6
5	0.3	45	55	6
10	0.3	45	55	6
18	0.3	10	90	1

Table S3 Parameter settings of Mass Spectroscopy for 2-PG and 3-PGA measurement.

Mass Spectroscopy conditions	Parameter settings
Voltage of capillary	3.0 (kV)
Temperature of desolvation gas	500 (℃)
Flow rate of desolvation gas	1000 (L/h)
Voltage of desolvation gas	25 (kV)
Collision energy	15 (eV)
Flow rate of cone hole	150 (L/h)
Ion source voltage	150 (℃)

Table S4 The secondary structure changes of Rubisco after binding with Cd^{2+}.

Rubisco:Cd	helix1	helix2	α- helix	β-turn	unordered
Rubisco (5μmol/L)	19.7	17.3	37.0	14.7	41.4
Rubisco: Cd = 1:2	22.0	20.1	42.1	14.7	43.2
Rubisco: Cd = 1:4	14.5	19.8	34.3	16.8	48.9
Rubisco: Cd = 1:6	16.3	20.2	36.5	14.4	49.1
Rubisco: Cd = 1:8	17.8	21.7	39.5	14.1	46.4

Table S5 Thermodynamic parameters of binding.

Parameters	Cd^{2+}	Mg^{2+}	Cd^{2+} + RuBP	Mg^{2+} + RuBP
K_a (L/μmol)	0.374	2.50	14.5	6.87
K_d (μmol/L)	2.67	0.40	690	14.6
n	1.37	1.03	1.72	2.05
ΔH (kJ/mol)	46.1	−2.56	−19.7	−7.88
ΔS (J/(mol·K))	261	113	13.5	47.0
ΔG (kJ/mol)	−31.8	−36.4	−21.9	−23.8

Table S6 The binding force and bond length of interactions between metal and Rubisco.

Metals	Atomic radii (Å)	Ionic radii (Å)	Nuclear charges	Bond length (Å)	Binding energy (kJ/mol)
Ni	1.15	0.69	28	2.10	−58.70
Mg	1.36	0.72	12	2.06	−47.07
Cu	1.17	0.73	29	2.45	−43.77
Cd	1.48	0.95	48	2.27	−23.09
Hg	1.49	1.02	80	2.53	−13.61

Table S7 The MMPBSA analysis of Cd^{2+}/Mg^{2+}-Rubisco-RuBP complex.

Energy types	Cd^{2+}-Rubisco-RuBP	Mg^{2+}-Rubisco-RuBP
Van der Waals Energy (kJ/mol)	−96.411	−84.699
Electrostatic energy (kJ/mol)	−195.534	−233.280
Polar solvation energy (kJ/mol)	252.302	278.774
SASA Energy (kJ/mol)	−16.968	−13.862
Total Binding Energy (kJ/mol)	−56.611	−53.067

Table S8 Changes of metabolite content under the stresses of Cd (μg/L).

Category	KEGG ID	Metabolite name	10	50	100	500
Sugar	C00031	D-Glucose	1.49	1.43	1.54	1.46
	C00089	Sucrose	0.95	0.88	0.56	0.48
	C00095	D-Fructose	0.35	0.32	0.47	0.84
	C00124	D-Galactose	1.37	1.59	1.71*	2.11**
	C00159	D-Mannose	1.65*	1.02	1.67*	1.01
	C00181	D-Xylose	3.65**	3.39**	2.5**	3.61**
	C00216	D-Arabinose	0.96	0.71	0.91	0.94
	C08235	D-Talopyranose	1.49	1.09	0.83	0.75
	C01728	2-alpha-Mannobiose	3.39**	3.24**	2.88**	3.18**
	C06115	Arabinofuranose	1.01	1.13	1.28	0.82
Amino acid	C00025	L-Glutamic acid	1.14	1.18	0.73	1.02
	C00037	Glycine	2.02**	3.1**	2.58**	3.21**
	C00041	L-Alanine	3.34**	2.55**	3.32**	3.13**
	C00049	L-Leucine	3.27**	2.28**	6.04**	2.51**
	C00065	L-Serine	3.16**	2.52**	4.65**	5.84**
	C00183	L-Valine	4.08**	6.65**	8.09**	5.74**
	C00188	L-Threonine	8.36**	6.42**	9.04**	8.52**
	C01879	L-5-Oxoproline	0.75	1.68*	2.11**	3.63**

	C00042	Succinic acid	2.14**	1.14	1.19	0.78
	C00048	Glyoxylate	4.46**	4.53**	7.89**	2.17**
	C00122	Formate	2.02	3.10	2.58	3.21
	C00149	Malic acid	2.45**	1.73*	1.72*	1.77*
	C00158	Citric acid	4.75**	3.66**	2.7**	2.18**
	C00160	Glycolate	1.7*	1.47	4.25**	2.11**
	C00168	Hydroxypyruvic acid	1.28	0.97	1.01	0.76
	C00186	L-Lactic acid	0.62*	0.53*	0.64*	1.21
Organic acid	C00009	Phosphoric acid	1.83	1.35	1.34	1.14
	C00209	Oxalate	6.65**	6.1**	2.69**	4.45**
	C00246	Butanoic acid	1.53	1.13	1.28	1.07
	C00257	D-Gluconic acid	0.70	0.69	0.71	0.61*
	C00258	Glycerate	2.11**	1.23	1.58	1.18
	C00296	Quinic acid	0.55*	0.77	0.85	1.14
	C01732	2-Butenedioic acid	1.79*	1.37	1.53	1.43
	C00493	Shikimic acid	0.63*	0.68	0.79	0.80
	C00898	Tartaric acid	0.63*	1.13	2.93**	0.65*
	C00249	Palmitic Acid	1.15	0.97	1.08	0.82
	C00333	Octadecadienoic acid	1.38	0.67*	1.09	0.77
Fatty acid	C00811	4-Coumaric acid	1.18	1.37	1.29	1.24
	C01530	Stearic acid	1.2	1.13	1.06	0.91
	C06427	alpha-Linolenic acid	1.19	0.86	0.97	0.82

Secondary metabolites	C00137	Myo-Inositol	1.34	0.87	1.01	0.84
	C00189	Ethanolamine	2.16**	1.46	1.36	1.52
	C00469	Ethanol	1.86*	1.31	1.27	1.18
	C00503	Erythritol	0.45*	0.72	0.74	0.68
	C01389	Phytol	1.43	1.15	0.86	0.60*
	C01789	Campesterol	1.47	1.13	1.07	0.91
	C02477	alpha-Tocopherol	1.97	1.48	1.38	1.10
	C03619	Galactoside	2.67**	1.32	1.45	0.92
	C05442	Stigmasterol	1.37	1.11	1.05	0.89
	C06400	D-Glucopyranoside	1.69	1.48	3.27**	0.66*
	C00116	Glycerol	0.44**	0.67*	0.93	0.57*
	C09771	Aucubin	0.91	0.84	1.70*	0.76

NS, $p > 0.05$; *, $p < 0.05$; **, $p < 0$.